ELSEVIER

International Journal of Pharmaceutics 140 (1996) 185–193

international journal of pharmaceutics

Porosity expansion of tablets as a result of bonding and deformation of particulate solids

K. van der Voort Maarschalk[a,*], K. Zuurman[a], H. Vromans[b], G.K. Bolhuis[a], C.F. Lerk[a]

[a]*Department of Pharmaceutical Technology and Biopharmacy, University of Groningen, Antonius Deusinglaan 1, 9713 AV Groningen, The Netherlands*
[b]*N.V. Organon, Oss, The Netherlands*

Received 11 March 1996; accepted 1 May 1996

Abstract

This paper describes the tabletting process of γ-sorbitol on the basis of the stress-deformation curve. This curve distinguishes between small, elastic deformation and large, viscous deformation. Small deformations can be quantified by the dynamic Young's modulus. The results demonstrated an effect of both rate of strain and initial particle size on the Young's modulus. The yield strength of compacts is a quantification of large deformations. There appeared to be an effect of strain rate on yield strength, but no clear relation between initial particle size and yield strength. The study relates elastic deformation with storage of elastic energy. The amount of stored energy was found to increase with compaction speed, and is postulated to be the driving force for changes of tablet porosities after compression. The attraction between particles causes resistance against porosity expansion, and is defined as expansion capacity. The expansion capacity showed no relation to compaction speed. It is therefore concluded that the effect of compaction speed on tablet properties is purely an effect of the amount of stored energy. The reciprocal value of expansion capacity demonstrated a direct relation with the constant that fits the relation between tablet strength and porosity. The expansion capacity is hence a quantification of bonding.

Keywords: Porosity; Relaxation; Sorbitol; Tablets; Yield strength; Young's modulus

1. Introduction

Tablets are formed by compaction of particulate materials. The sequence of events during the densification of powders is classically presented as particle rearrangement, plastic and elastic defor-

* Corresponding author.

PII S0378-5173(96)04584-X

mation and fragmentation of particles (Duberg and Nyström, 1986). This is in fact what is described by the stress–strain curve as known in polymer mechanics (Crawford, 1987). This curve expresses the relation between strain and stress that is necessary to reach that deformation. At small deformations, the material behaves elastically (according to Hooke's law). At a specific deformation, with corresponding stress (the yield point), the material starts to deform viscously, i.e. stress does not increase with further deformation. At even larger deformation, the material breaks. In tabletting practice, materials are usually referred to as either brittle or plastic due to their predominant deformation behaviour. However, this does not mean that only these deformation mechanisms occur. For example, even brittle materials exhibit a certain plastic or elastic component. The term plastic deformation is basically too simple and could better be replaced by viscoelastic deformation. The fact that tabletting speed affects the consolidation behaviour is a result of viscoelasticity.

A number of papers have been published aiming to relate tabletting behaviour with the properties of the material to be compacted, as summarized by Doelker (1993). The most extensively studied material properties are the elastic or Young's modulus and the yield strength. The most common method to measure the elastic modulus makes use of bending techniques on massive strips. As a compact is not a massive strip, values obtained at various porosity levels are extrapolated to zero porosity. The outcome is thought to represent the elastic modulus of the material (Bassam et al., 1988). A frequently applied method to study irreversible particle deformation is the Heckel porosity function, from which the yield strength can be derived (Heckel, 1961a,b).

This study was performed to relate both particle deformation and bonding to porosity expansion of the tablets compacted. Different parameters are distinguished and quantified.

2. Experimental

2.1. Theoretical background

In dynamic mechanical analysis (DMA) a small sinusoidal strain is imparted to a sample with a frequency (f). If the test material is completely elastic, the deformation and the stress that is necessary to cause the deformation are directly proportional. In the case of completely viscous materials, the applied stress is not dependent on the strain, but on the rate of strain. As a result of the periodical (sinusoidal) deformation, a phase-shift (δ) exists between deformation and stress. The phase-shift of purely viscous materials is $\frac{1}{2}\pi$ rad, whereas the phase-shift of completely elastic materials is 0 rad. Materials with intermediate, so-called viscoelastic deformation behaviours, exhibit a phase-shift between 0 and $\frac{1}{2}\pi$ rad.

It is possible to characterize the deformation properties of materials with two parameters. The first is the complex modulus (E^*), sometimes called the dynamic Young's modulus, which quantifies the stiffness of the material. The complex modulus is the ratio of the maximum stress (σ_{max}) to the maximum deformation (γ_{max})

$$E^*(f) = \frac{\sigma_{max}(f)}{\gamma_{max}(f)} \tag{1}$$

The second parameter is the damping, which quantifies the viscoelasticity of the test material. It is the tangent of the phase-shift (tan (δ)). In practice, both the complex modulus and the damping depend upon the deformation rate.

The occurrence of a phase-shift implies that the complex modulus consists of two parts: the storage modulus (E'), quantifying the elastically stored energy, and the loss modulus (E''), quantifying the energy dissipation. The elastic moduli are interrelated by

$$E^* = \sqrt{E'^2 + E''^2} \tag{2}$$

The damping is related to the storage and loss modulus by

$$\tan(\delta) = \frac{E''}{E'} \tag{3}$$

It is known that the damping is a quantification of the viscoelasticity of materials (Cowie, 1991).

2.2. Experiments

The material used was spray-dried sorbitol (Karion® Instant, Merck, Darmstadt, Germany). All fractions, apart from the coarsest fraction, were obtained by milling the powder in a Fritsch mill (Idar Oberstein, Germany). The milled samples were sieved with an Alpine Air Jet Sieve (Augsburg, Germany) using USA Standard testing sieves (W.B. Tyler Inc., Mentor, OH, USA). The smallest fraction was obtained with an air classifier (Alpine Multiplex Labor Zickzacksichter 100 MR).

The average particle sizes of the sieve fractions were measured with a Sympatec Helos particle size analyser (Haan, Clausthal, Germany). The specific surface area (A_{sp}) was calculated from the particle size distribution of each sieve fraction with

$$A_{sp} = \frac{6}{\rho \cdot < d_p >} \tag{4}$$

where A_{sp} is the specific surface area of a sieve fraction, ρ is the true density of the material and $< d_p >$ is the particle size distribution of that sieve fraction.

True density of the material was measured at a temperature of 22°C by helium pycnometry with a Quantachrome pycnometer (Syosset, USA). The true density of sorbitol is 1488 kg m^{-3}.

Viscoelastic properties were assessed by dynamic mechanical analysis (DMA) with a Rheometrics Solids Analyzer (Piscataway, NJ, USA), using the dual cantilever method. The method was described in detail in a previous paper (Van der Voort Maarschalk et al., 1996). Strips of the test material of a size of about 60 × 6 × 1 mm were prepared with a hand press (Paul Weber, Stuttgart, Germany) in a specially designed punch-and-die set. The maximum applied pressure varied between 15 and 370 MPa and was held constant for about 10 s. After ejection and a relaxation period of at least 16 h the size of the strips was measured with an electronic micrometer (Mitutoyo, Tokyo, Japan) and weighed on an analytical balance (Mettler, Zürich, Switzerland). The maximum strain in the experiments was 0.01%. The measurement started at a frequency of 0.1 rad s^{-1} and ended at a frequency of 100 rad s^{-1}.

Flat-faced compacts of 500 mg and a diameter of 13 mm were prepared on a high speed compaction simulator (ESH, Brierley Hill, UK) at a temperature of 22°C and a relative humidity of 60%. The maximum applied pressures varied between about 5 and 350 MPa. The upper punch displacement profiles were sine-waves with different amplitudes in order to reach different maximum compression pressures. As sinusoidal profiles were used, a complete profile involves π rad. Knowing both the compression speed (v) and the penetration depth (A_{comp}), it is possible to calculate the angular frequency of the compression (f)

$$f = \frac{\pi \cdot v}{2 \cdot A_{comp}} \tag{5}$$

which makes it possible to correlate DMA to compaction experiments. Three average compaction speeds (3, 30 and 300 mm s^{-1}) were choosen within the range of angular frequencies 0.1 and 100 rad s^{-1} (as applied for the DMA measurements). The lower punch was stationary during compression. The ejection time was always 10 s. Both upper punch and lower punch displacement and force were recorded. The resolution of the analogue-to-digital conversion was 0.3 μm, the total error of the measurements appeared to be better than $\pm$ 10 μm. Corrections were made for elastic punch deformation. Before each compression cycle the die was lubricated with magnesium stearate. After a relaxation period of at least 16 h, tablet dimensions were measured with the micrometer and weighed on the analytical balance. The crushing strength of the tablets was measured with the compaction simulator. Profiles with a linear speed of 0.25 mm s^{-1} were created, and the maximum applied pressure was recorded on an XY-recorder (Kipp and Zonen, Delft, The Netherlands). The tensile strength of the tablets was calculated according to Fell and Newton (1968).

3. Results and discussion

3.1. Deformation of the test material

The viscoelastic parameter profiles of porous compacts, compressed from the different sieve fractions of sorbitol, were measured at different rates of deformation. As the voidage of the compacts influences the values of the parameters, measurements were performed at different porosities. The elastic moduli at a porosity of zero were achieved by extrapolation as previously described (Van der Voort Maarschalk et al., 1996). Fig. 1a indicates that the complex modulus increases with both deformation rate and decreasing particle size. Despite the large confidence intervals of the experimental data (illustrated for compacts made from sieve fraction 53–75 μm at a frequency of 1 rad s^{-1}), the figure demonstrates increasing complex moduli with decreasing initial particle size. This result is not evident for reason that extrapolation of the complex modulus to zero porosity is thought to yield the material properties (Bassam et al., 1988). However, the observed dependence of the complex modulus on the initial particle size may be explained if it is realized that the resistance against deformation of a compact is the result of the rigidity of the particles themselves and the total number of bonds between all particles. Where interparticle bonding increases with decreasing particle size, deformation of the compact will increasingly be affected by deformation of the particles themselves, giving highest complex moduli for the compacts compressed from the finest particle size fraction. Thus, the complex modulus of the material will best be represented by the data as obtained for the compacts compressed from the smallest particle size fraction and extrapolated to zero porosity.

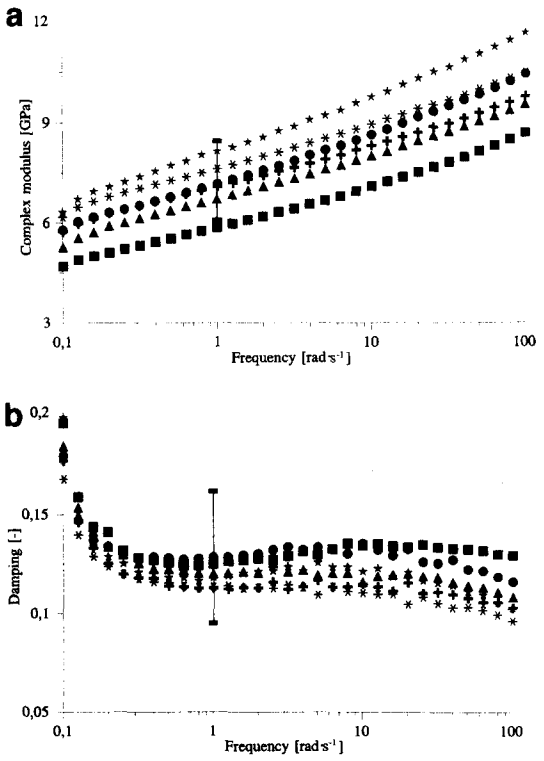

Fig. 1. Calculated complex modulus (1a) and damping (1b) at zero porosity as a function of the rate of deformation of compacts compressed from different sieve fractions. Symbols: (✱) <25 μm, (●) 53–75 μm, (*) 75–106 μm, (+) 106–149 μm, (▲) 212–300 μm, (■) 600–850 μm. The error bars give the 95% confidence intervals of compacts produced from particles of 53–75 μm at a frequency of 1 rad s^{-1}.

Values of the damping vary between 0.1 and 0.2 depending upon rate of deformation (Fig. 1b). As the storage modulus is about one order of magnitude larger than the loss modulus, it is concluded that the material is merely elastic at small deformations. Moreover, it is noted that calculation of the damping causes an increase in relative error, as illustrated in Fig. 1b for the compacts made from sieve fraction 53–75 μm. Consequently, no significant effect of particle size is shown.

DMA is a technique that measures at small strains, and the changes of deformation are mainly reversible as indicated by low values of the damping. On the contrary, consolidation really forces a material to deform largely, resulting into permanent changes of shape of the material. The outcomes of the two distinct methods (DMA and consolidation) cannot be superposed, but can rather more be considered to complement each other. This is elucidated in Fig. 2, which is the representation of the stress–strain curve. The solid line represents the stress–strain relation of viscoelastic materials. At small deformations, the material behaves like a mainly elastic solid, and stress and strain are proportional. The propor-

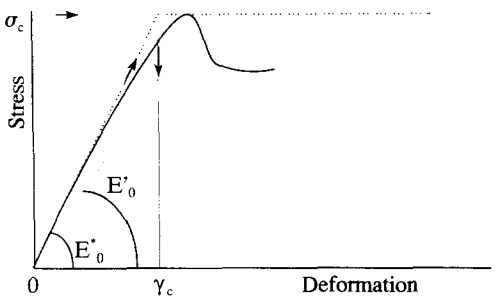

Fig. 2. Stress-deformation relation (solid line), simplified relation (dotted line) and energy storage of viscoelastic materials.

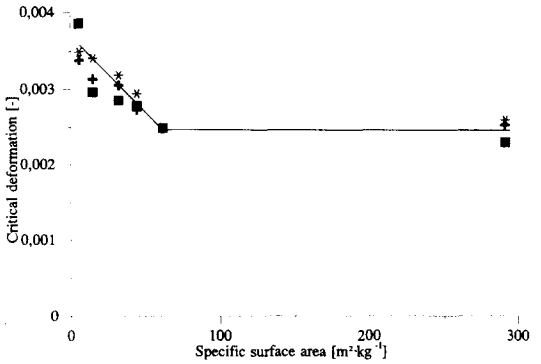

Fig. 3. Critical deformation of the test materials as a function of the specific surface area at different rates of compaction. Symbols: (■) 3 mm s^{-1}, (+) 30 mm s^{-1}, (*) 300 mm s^{-1}.

tionality constant equals the complex modulus and depends on the rate of strain. At larger strain, stress reaches a maximum value, the yield strength (σ_c). Behind this point, the material behaves rather as a viscous than as an elastic solid. Values for yield strength (σ_c) can be derived from Heckel-plots (ln porosity versus pressure) using an emperical relationship between slope (K) of the linear part of the plot and yield strength, as indicated by Heckel (1961a,b)

$$\sigma_c = \frac{1}{3 \cdot K} \tag{6}$$

The values of the yield strength of the different sieve fractions as calculated from Heckel-curves at different compression speeds are depicted in Table 1. The table shows a direct relation between compaction speed and yield strength. On the contrary, no relation is shown between the yield strength and the initial particle size. Yield of a material is obviously rather a material characterisation than a property of particulate matter here.

Table 1
Yield strengths [MPa] of the test materials at different compaction speeds

Sieve fraction (μm)	Speed (mm s^{-1})		
	3	30	300
<25	18	24	29
53–75	17	21	25
75–106	21	24	30
106–149	20	25	30
212–300	19	24	31
600–850	22	23	29

Knowing both the complex modulus (from DMA measurements) and the yield strength (from compaction experiments), it is possible to derive a simplified stress–deformation curve by plotting a straight line with slope E_0^* up to yield strength σ_c (Fig. 2, dotted line). From this point the substance deforms plastically, where further deformation does not result in additional stress. The corresponding strain, the 'critical deformation' (γ_c), can be derived by

$$\gamma_c = \frac{\sigma_c}{E_0^*} \tag{7}$$

Fig. 3 shows the relation between the calculated critical deformation and the specific surface area of the initial particles, plotted for the three compaction speeds (3, 30 and 300 mm s^{-1}). It is noticed that the critical deformation values are small; yield takes place when the deformation is between 0.0025 and 0.0040.

The simplified stress–deformation curve (Fig. 2) also gives the possibility to calculate the amount of elastically stored energy. At deformations exceeding γ_c, viscous flow (yield) takes place. If it is assumed that no extra energy storage takes place at deformations larger than the critical deformation, and the stress–strain curve is simplified into the one as presented by the dotted line in Fig. 2, the amount of elastically stored energy (W_{rev}) can by calculated as:

$$W_{rev} = \int_0^{\gamma_c} E_0^* \cdot \gamma d\gamma = \frac{1}{2} \cdot \sqrt{\frac{E_0^{*2}}{1 + \tan^2\delta}} \cdot \gamma_c^2 \quad (8)$$

corresponding with the shaded area in Fig. 2. Table 2 lists the calculated energy storage on compaction of different sorbitol fractions at different compaction speeds. The data indicate no significant effect of the initial particle size but demonstrate increasing amount of stored energy with increasing compaction speed.

3.2. Porosity expansion of tablets

Relaxation of tablets is often quantified as an increase in volume, or tablet height after compression (Doelker, 1993). This expansion principally is a result of two different phenomena. On the one hand, compaction always leads to a certain extent of material compression, expressed as an increase in true density (ρ), which is fully reversible. On the other hand, there is a built up of elastic energy which is responsible for the increase in porosity of a compact in the relaxation period.

The porosity expansion ($\Delta\epsilon$) after compression was calculated according to

$$\Delta\epsilon = \epsilon - \epsilon_{min} \quad (9)$$

with ϵ the tablet porosity after relaxation and ϵ_{min} the minimum attainable porosity under pressure (often zero in the experimental conditions). Fig. 4 depicts the porosity expansion of compacts compressed at different speeds of compaction from a representative sieve fraction (75–106 μm) of sorbitol. The porosity expansion appears to be almost constant. The larger values at pressures of about 200 MPa are due to material compression. Even if the calculated porosity under pressure has a positive value, there is a certain amount of material compression, causing a low value of porosity, and hence larger values of porosity expansion. The results show highest porosity expansions for the compacts compressed at the highest compaction speed.

Table 2
Calculated stored energies (kJ m^{-3}) of spray-dried sorbitol compacts at different compaction speeds

Sieve fraction (μm)	Speed ($mm \cdot s^{-1}$)		
	3	30	300
<25	20	33	54
53–75	21	25	42
75–106	29	32	54
106–149	28	38	61
212–300	28	40	66
600–850	42	42	72

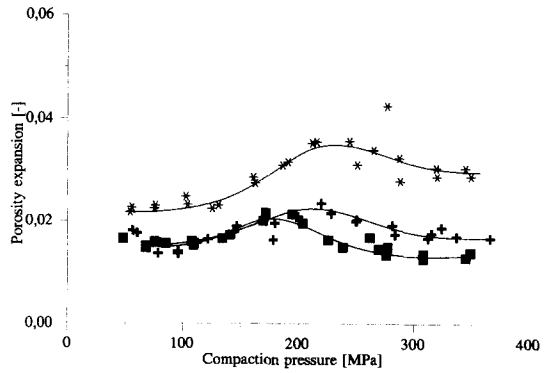

Fig. 4. Porosity expansion as a function of the compaction pressure of tablets compressed from sieve fraction 75–106 μm at different compaction speeds. Symbols as in Fig. 3.

Porosity expansion of a tablet is the final result of relaxation, whereas the amount of elastically stored energy can be regarded as the driving force for that relaxation. In Fig. 5 porosity expansion is plotted versus that driving force cq. the amount of stored energy. The stored energy was calculated according Eq. (8). The figure points to different

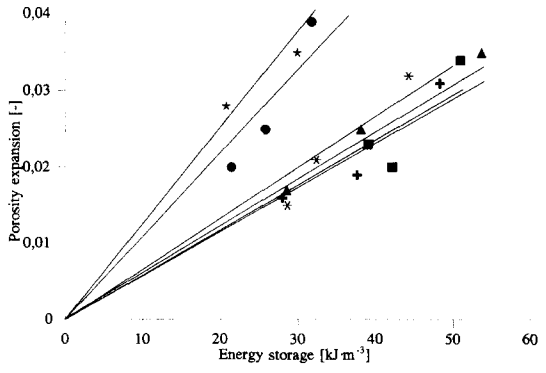

Fig. 5. Porosity expansion as a function of the calculated energy storage. Symbols as in Fig. 1.

Table 3
Expansion capacities of tablets compressed from different sieve fractions γ-sorbitol

Sieve fraction (μm)	Expansion capacity (*10^{-6} m^3 J^{-1})
<25	1.14
53–75	1.09
75–106	0.66
106–149	0.59
212–300	0.65
600–850	0.59

relaxation properties for the different sieve fractions; tablets compressed from smaller particles exhibit larger porosity expansions than tablets compressed from larger particles. Realizing again that porosity expansion is the nett result of an interaction between a driving force (elastic energy storage) and the resistance against creation of a porous structure, the proportionality constant (p_{exp}) between porosity expansion and energy storage is introduced as 'expansion capacity',

$$\frac{\Delta\epsilon}{W_{rev}} = p_{exp} \tag{10}$$

Plotting straight lines through the experimental data for each sieve fraction, the obtained expansion capacities are listed in Table 3 for the different particle size fractions.

3.3. Tensile strength of tablets

The mechanical properties of a tablet are the consequence of consolidation and expansion phenomena. Fig. 6 depicts the relation between tensile strength and porosity of tablets compresssed at different compaction speeds from a representative sample (fraction 75–106 μm) of sorbitol. A unique relationship is found to exist between strength and porosity of the tablets, independent of the speed of compression. Similar, but numerically different, profiles were obtained for tablets compressed from other particle size fractions. All profiles were fitted according to the Ryskewitch-Duckworth relation (Duckworth, 1953),

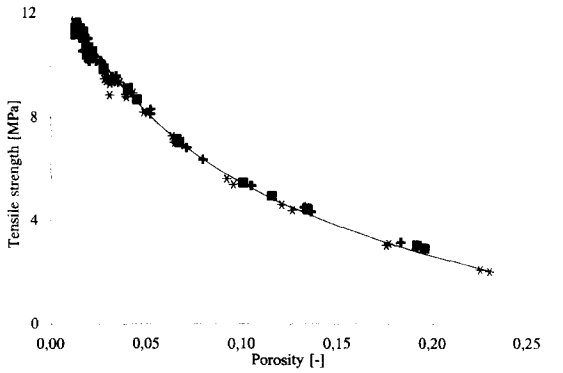

Fig. 6. Tensile strength as a function of the tablet porosity of tablets compressed from sieve fraction 75–106 μm at different compaction speeds. Symbols as in Fig. 3.

$$\ln\frac{S}{S_0} = -k \cdot \epsilon \tag{11}$$

where S is the tensile strength, S_0 the tensile strength at zero porosity, ϵ the porosity of the tablets and k a constant. High values of k indicate that tablet strength increases rapidly with decreasing porosity, pointing to stronger bonding of the particles. Parameter k is consequently called 'bonding capacity'. Calculated values for k with corresponding tensile strengths at zero porosity (S_0) are listed in Table 4. The data indicate lower bonding for the smaller particle size fractions. This result agrees with increasing tensile strength (at zero porosity) with increasing particle size. The calculated tensile strength at zero porosity is therefore not a property of the material, as reported earlier by Svensson et al. (1994).

Table 4
Fit parameters from Ryskewitch-Duckworth relation

Sieve fraction (μm)	k(–)	S_0 (MPa)
<25	5.20	9.1
53–75	6.94	8.6
75–106	10.87	9.5
106–149	7.74	12.2
212–300	8.61	11.7
600–850	8.95	12.0

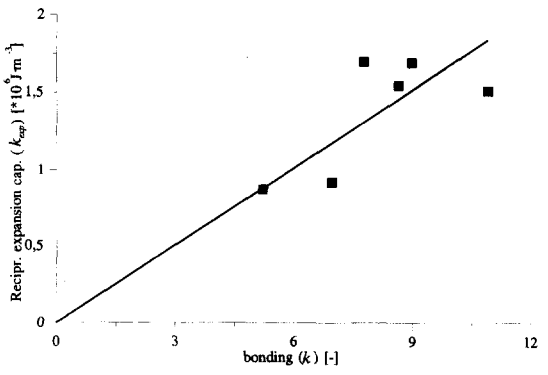

Fig. 7. Reciprocal expansion capacity (k_{exp}^{-1}) as a function of bonding (k).

3.4. Porosity expansion and bonding

Fig. 5 suggests that the release of a certain amount of elastic energy is unequivocally related to porosity expansion of a particulate tablet. The amount of stored energy is hence the driving force for relaxation of tablets. The proportionality constant (p_{exp}) between porosity expansion and energy storage has consequently been introduced as expansion capacity of the compact after compression. Different expansion capacities were found for the different initial particle sizes (Table 3). Realizing that expansion is counteracted by bonding, the reciprocal expansion capacity (p_{exp}^{-1}) can be regarded as a measure for bonding. But, bonding is also expressed by the tensile strength of a tablet and can be characterized by bonding capacity (k), as derived from the Ryskewitch-Duckworth relation (Table 4).

These considerations suggest a direct relation between the reciprocal expansion capacity (p_{exp}^{-1}) and the bonding parameter (k). Fig. 7 indeed proves the existence of that direct relation.

4. Conclusion

It is concluded that the increase in porosity of tablets is the nett result of a driving force (stored energy) that causes relaxation and particle bonding that prevents a tablet from relaxation. The driving force for relaxation is quantified by the amount of stored energy, increasing with compaction speed. The proportionality constant between porosity expansion and energy storage is called expansion capacity and decreases with increasing particle size of the powder to be compacted. The reciprocal expansion capacity can be regarded as a parameter for bonding and is indeed found to correlate directly with the bonding parameter as derived from the fit-constant of the Ryskewitch-Duckworth relation. The direct relation between expansion and bonding capacity enables prediction of the compactibility of powders from porosity expansion of tablets and conversely.

The phenomenon of more porous tablets on increasing compaction speed is explained by increasing amounts of stored energy.

5. Symbols

A_{comp}	penetration depth
A_{sp}	specific surface area
$<d_p>$	particle size distribution
E' (E'_0)	storage modulus (at zero porosity)
E''	loss modulus
E^* (E^*_0)	complex modulus (at zero porosity)
f	frequency
k	constant, bonding capacity
K	constant
p	pressure
S (S_0)	tensile strength (at zero porsity)
W_{rev}	energy storage
γ	deformation
γ_c	critical deformation
δ	phase shift
ϵ	porosity
ϵ_{min}	minimum porosity under pressure
$\Delta\epsilon$	porosity expansion
ρ	true density
σ	stress
σ_c	yield strength

References

Bassam, F., York, P., Rowe, R.C. and Roberts, R.J., Effect of particle size and source on variability of Young's modulus

of microcrystalline cellulose powders. *J. Pharm. Pharmacol.*, 40 (1988) 68P.

Cowie, J.M.G., *Polymers: Chemistry & Physics of Modern Materials*, 2nd edn., Blackie, London, 1991.

Crawford, R.J. *Plastics Engineering*, 2nd edn., Pergamon, Oxford, 1987.

Doelker, E., Comparative compaction properties of various microcrystalline cellulose types and generic products. *Drug Dev. Ind. Pharm.*, 19 (1993) 2399–2471.

Duberg, M. and Nyström, C., Studies on direct compression of tablets XVII. Porosity-pressure curves for the characterization of volume reduction mechanismes in powder compression. *Powder Technol.*, 46 (1986) 67–75.

Duckworth, W.H., Discussion of Ryshkewitch paper by Winston Duckworth *J. Am. Ceram. Soc.*, 36 (1953) 68.

Fell, J.T. and Newton, J.M., The tensile strength of lactose tablets. *J. Pharm. Pharmacol.*, 20 (1968) 657–658.

Heckel, R.W., Density-pressure relationships in powder compaction. *Trans. Met. Soc. AIME.*, 221 (1961a) 671–675.

Heckel, R.W., An analysis of powder compaction phenomena. *Trans. Met. Soc. AIME.*, 221 (1961b) 1001–1008.

Svensson, Å., Alderborn, G. and Nyström, C., Effect of particle size and post compaction storage time on the tensile strength of compacts, at zero porosity, obtained by specimen values. *Abstracts of the Int. Symp. on Solid Dosage Forms*, Stockholm, 1994, p. 30.

Van der Voort Maarschalk, K., Vromans, H., Bolhuis, G.K., Lerk, C.F., The effect of viscoelasticity and tabletting speed on consolidation and relaxation of a viscoelastic material. *Eur. J. Pharm. Biopharm.*, 42 (1996) 49–55.